

UC Berkeley

UC Berkeley Previously Published Works

Title

Measurement of B^0 - B^0 Flavor Oscillations in Hadronic B^0 Decays

Permalink

<https://escholarship.org/uc/item/0mr3j0mp>

Journal

Physical Review Letters, 88(22)

ISSN

0031-9007

Authors

Aubert, B
Boutigny, D
Gaillard, J-M
[et al.](#)

Publication Date

2002-06-03

DOI

10.1103/physrevlett.88.221802

Copyright Information

This work is made available under the terms of a Creative Commons Attribution License, available at <https://creativecommons.org/licenses/by/4.0/>

Peer reviewed

Measurement of $B^0\text{-}\bar{B}^0$ Flavor Oscillations in Hadronic B^0 Decays

B. Aubert,¹ D. Boutigny,¹ J.-M. Gaillard,¹ A. Hicheur,¹ Y. Karyotakis,¹ J.P. Lees,¹ P. Robbe,¹ V. Tisserand,¹
 A. Palano,² A. Pompili,² G.P. Chen,³ J.C. Chen,³ N.D. Qi,³ G. Rong,³ P. Wang,³ Y.S. Zhu,³ G. Eigen,⁴ B. Stugu,⁴
 G.S. Abrams,⁵ A.W. Borgland,⁵ A.B. Breon,⁵ D.N. Brown,⁵ J. Button-Shafer,⁵ R.N. Cahn,⁵ A.R. Clark,⁵ M.S. Gill,⁵
 A.V. Gritsan,⁵ Y. Groysman,⁵ R.G. Jacobsen,⁵ R.W. Kadel,⁵ J. Kadyk,⁵ L.T. Kerth,⁵ Yu.G. Kolomensky,⁵ J.F. Kral,⁵
 C. LeClerc,⁵ M.E. Levi,⁵ G. Lynch,⁵ P.J. Oddone,⁵ M. Pripstein,⁵ N.A. Roe,⁵ A. Romosan,⁵ M.T. Ronan,⁵
 V.G. Shelkov,⁵ A.V. Telnov,⁵ W.A. Wenzel,⁵ T.J. Harrison,⁶ C.M. Hawkes,⁶ D.J. Knowles,⁶ S.W. O'Neale,⁶
 R.C. Penny,⁶ A.T. Watson,⁶ N.K. Watson,⁶ T. Deppermann,⁷ K. Goetzen,⁷ H. Koch,⁷ M. Kunze,⁷ B. Lewandowski,⁷
 K. Peters,⁷ H. Schmuecker,⁷ M. Steinke,⁷ N.R. Barlow,⁸ W. Bhimji,⁸ N. Chevalier,⁸ P.J. Clark,⁸ W.N. Cottingham,⁸
 B. Foster,⁸ C. Mackay,⁸ F.F. Wilson,⁸ K. Abe,⁹ C. Hearty,⁹ T.S. Mattison,⁹ J.A. McKenna,⁹ D. Thiessen,⁹ S. Jolly,¹⁰
 A.K. McKemey,¹⁰ V.E. Blinov,¹¹ A.D. Bukin,¹¹ D.A. Bukin,¹¹ A.R. Buzykaev,¹¹ V.B. Golubev,¹¹ V.N. Ivanchenko,¹¹
 A.A. Korol,¹¹ E.A. Kravchenko,¹¹ A.P. Onuchin,¹¹ S.I. Serednyakov,¹¹ Yu.I. Skovpen,¹¹ V.I. Telnov,¹¹
 A.N. Yushkov,¹¹ D. Best,¹² M. Chao,¹² D. Kirkby,¹² A.J. Lankford,¹² M. Mandelkern,¹² S. McMahon,¹² D.P. Stoker,¹²
 K. Arisaka,¹³ C. Buchanan,¹³ S. Chun,¹³ D.B. MacFarlane,¹⁴ S. Prell,¹⁴ Sh. Rahatlou,¹⁴ G. Raven,¹⁴ V. Sharma,¹⁴
 C. Campagnari,¹⁵ B. Dahmes,¹⁵ P.A. Hart,¹⁵ N. Kuznetsova,¹⁵ S.L. Levy,¹⁵ O. Long,¹⁵ A. Lu,¹⁵ J.D. Richman,¹⁵
 W. Verkerke,¹⁵ J. Beringer,¹⁶ A.M. Eisner,¹⁶ M. Grothe,¹⁶ C.A. Heusch,¹⁶ W.S. Lockman,¹⁶ T. Pulliam,¹⁶ T. Schalk,¹⁶
 R.E. Schmitz,¹⁶ B.A. Schumm,¹⁶ A. Seiden,¹⁶ M. Turri,¹⁶ W. Walkowiak,¹⁶ D.C. Williams,¹⁶ M.G. Wilson,¹⁶
 E. Chen,¹⁷ G.P. Dubois-Felsmann,¹⁷ A. Dvoretzki,¹⁷ D.G. Hitlin,¹⁷ S. Metzler,¹⁷ J. Oyang,¹⁷ F.C. Porter,¹⁷ A. Ryd,¹⁷
 A. Samuel,¹⁷ M. Weaver,¹⁷ S. Yang,¹⁷ R.Y. Zhu,¹⁷ S. Devmal,¹⁸ T.L. Geld,¹⁸ S. Jayatilke,¹⁸ G. Mancinelli,¹⁸
 B.T. Meadows,¹⁸ M.D. Sokoloff,¹⁸ T. Barillari,¹⁹ P. Bloom,¹⁹ M.O. Dima,¹⁹ W.T. Ford,¹⁹ U. Nauenberg,¹⁹
 A. Olivas,¹⁹ P. Rankin,¹⁹ J. Roy,¹⁹ J.G. Smith,¹⁹ W.C. van Hoek,¹⁹ J. Blouw,²⁰ J.L. Harton,²⁰ M. Krishnamurthy,²⁰
 A. Soffer,²⁰ W.H. Toki,²⁰ R.J. Wilson,²⁰ J. Zhang,²⁰ T. Brandt,²¹ J. Brose,²¹ T. Colberg,²¹ M. Dickopp,²¹
 R.S. Dubitzky,²¹ A. Hauke,²¹ E. Maly,²¹ R. Müller-Pfefferkorn,²¹ S. Otto,²¹ K.R. Schubert,²¹ R. Schwierz,²¹
 B. Spaan,²¹ L. Wilden,²¹ D. Bernard,²² G.R. Bonneaud,²² F. Brochard,²² J. Cohen-Tanugi,²² S. Ferrag,²²
 S. T'Jampens,²² Ch. Thiebaut,²² G. Vasileiadis,²² M. Verderi,²² A. Anjomshoa,²³ R. Bernet,²³ A. Khan,²³
 D. Lavin,²³ F. Muheim,²³ S. Playfer,²³ J.E. Swain,²³ J. Tinslay,²³ M. Falbo,²⁴ C. Borean,²⁵ C. Bozzi,²⁵ S. Dittongo,²⁵
 L. Piemontese,²⁵ E. Treadwell,²⁶ F. Anulli,^{27,*} R. Baldini-Feroli,²⁷ A. Calcaterra,²⁷ R. de Sangro,²⁷ D. Falciari,²⁷
 G. Finocchiaro,²⁷ P. Patteri,²⁷ I.M. Peruzzi,^{27,*} M. Piccolo,²⁷ Y. Xie,²⁷ A. Zallo,²⁷ S. Bagnasco,²⁸ A. Buzzo,²⁸
 R. Contri,²⁸ G. Crosetti,²⁸ M. Lo Vetere,²⁸ M. Macri,²⁸ M.R. Monge,²⁸ S. Passaggio,²⁸ F.C. Pastore,²⁸ C. Patrignani,²⁸
 M.G. Pia,²⁸ E. Robutti,²⁸ A. Santroni,²⁸ S. Tosi,²⁸ M. Morii,²⁹ R. Bartoldus,³⁰ R. Hamilton,³⁰ U. Mallik,³⁰
 J. Cochran,³¹ H.B. Crawley,³¹ P.-A. Fischer,³¹ J. Lamsa,³¹ W.T. Meyer,³¹ E.I. Rosenberg,³¹ G. Grosdidier,³²
 C. Hast,³² A. Höcker,³² H.M. Lacker,³² S. Laplace,³² V. Lepeltier,³² A.M. Lutz,³² S. Plaszczynski,³² M.H. Schune,³²
 S. Trincaz-Duvoid,³² G. Wormser,³² R.M. Bionta,³³ V. Brigljević,³³ D.J. Lange,³³ M. Mugge,³³ K. van Bibber,³³
 D.M. Wright,³³ A.J. Bevan,³⁴ J.R. Fry,³⁴ E. Gabathuler,³⁴ R. Gamet,³⁴ M. George,³⁴ M. Kay,³⁴ D.J. Payne,³⁴
 R.J. Sloane,³⁴ C. Touramanis,³⁴ M.L. Aspinwall,³⁵ D.A. Bowerman,³⁵ P.D. Dauncey,³⁵ U. Egede,³⁵ I. Eschrich,³⁵
 N.J.W. Gunawardane,³⁵ J.A. Nash,³⁵ P. Sanders,³⁵ D. Smith,³⁵ D.E. Azzopardi,³⁶ J.J. Back,³⁶ G. Bellodi,³⁶
 P. Dixon,³⁶ P.F. Harrison,³⁶ R.J.L. Potter,³⁶ H.W. Shorthouse,³⁶ P. Strother,³⁶ P.B. Vidal,³⁶ G. Cowan,³⁷ S. George,³⁷
 M.G. Green,³⁷ A. Kurup,³⁷ C.E. Marker,³⁷ P. McGrath,³⁷ T.R. McMahon,³⁷ S. Ricciardi,³⁷ F. Salvatore,³⁷ G. Vaitsas,³⁷
 D. Brown,³⁸ C.L. Davis,³⁸ J. Allison,³⁹ R.J. Barlow,³⁹ J.T. Boyd,³⁹ A.C. Forti,³⁹ J. Fullwood,³⁹ F. Jackson,³⁹
 G.D. Lafferty,³⁹ N. Savvas,³⁹ J.H. Weatherall,³⁹ J.C. Williams,³⁹ A. Farbin,⁴⁰ A. Jawahery,⁴⁰ V. Lillard,⁴⁰ J. Olsen,⁴⁰
 D.A. Roberts,⁴⁰ J.R. Schieck,⁴⁰ G. Blaylock,⁴¹ C. Dallapiccola,⁴¹ K.T. Flood,⁴¹ S.S. Hertzbach,⁴¹ R. Kofler,⁴¹
 V.B. Koptchev,⁴¹ T.B. Moore,⁴¹ H. Staengle,⁴¹ S. Willocq,⁴¹ B. Brau,⁴² R. Cowan,⁴² G. Sciolla,⁴² F. Taylor,⁴²
 R.K. Yamamoto,⁴² M. Milek,⁴³ P.M. Patel,⁴³ F. Palombo,⁴⁴ J.M. Bauer,⁴⁵ L. Cremaldi,⁴⁵ V. Eschenburg,⁴⁵
 R. Kroeger,⁴⁵ J. Reidy,⁴⁵ D.A. Sanders,⁴⁵ D.J. Summers,⁴⁵ J.Y. Nief,⁴⁶ P. Taras,⁴⁶ H. Nicholson,⁴ C. Cartaro,⁴⁸
 N. Cavallo,^{48,†} G. De Nardo,⁴⁸ F. Fabozzi,⁴⁸ C. Gatto,⁴⁸ L. Lista,⁴⁸ P. Paolucci,⁴⁸ D. Piccolo,⁴⁸ C. Sciacca,⁴⁸
 J.M. LoSecco,⁴⁹ J.R.G. Alsmiller,⁵⁰ T.A. Gabriel,⁵⁰ J. Brau,⁵¹ R. Frey,⁵¹ E. Grauges,⁵¹ M. Iwasaki,⁵¹ N.B. Sinev,⁵¹
 D. Strom,⁵¹ F. Colecchia,⁵² F. Dal Corso,⁵² A. Dorigo,⁵² F. Galeazzi,⁵² M. Margoni,⁵² G. Michelon,⁵² M. Morandin,⁵²
 M. Posocco,⁵² M. Rotondo,⁵² F. Simonetto,⁵² R. Stroili,⁵² E. Torassa,⁵² C. Voci,⁵² M. Benayoun,⁵³ H. Briand,⁵³
 J. Chauveau,⁵³ P. David,⁵³ Ch. de Vaissière,⁵³ L. Del Buono,⁵³ O. Hamon,⁵³ F. Le Diberder,⁵³ Ph. Leruste,⁵³

J. Ocariz,⁵³ L. Roos,⁵³ J. Stark,⁵³ P. F. Manfredi,⁵⁴ V. Re,⁵⁴ V. Speziali,⁵⁴ E. D. Frank,⁵⁵ L. Gladney,⁵⁵ Q. H. Guo,⁵⁵ J. Panetta,⁵⁵ C. Angelini,⁵⁶ G. Batignani,⁵⁶ S. Bettarini,⁵⁶ M. Bondioli,⁵⁶ F. Bucci,⁵⁶ E. Campagna,⁵⁶ M. Carpinelli,⁵⁶ F. Forti,⁵⁶ M. A. Giorgi,⁵⁶ A. Lusiani,⁵⁶ G. Marchiori,⁵⁶ F. Martinez-Vidal,⁵⁶ M. Morganti,⁵⁶ N. Neri,⁵⁶ E. Paoloni,⁵⁶ M. Rama,⁵⁶ G. Rizzo,⁵⁶ F. Sandrelli,⁵⁶ G. Simi,⁵⁶ G. Triggiani,⁵⁶ J. Walsh,⁵⁶ M. Haire,⁵⁷ D. Judd,⁵⁷ K. Paick,⁵⁷ L. Turnbull,⁵⁷ D. E. Wagoner,⁵⁷ J. Albert,⁵⁸ P. Elmer,⁵⁸ C. Lu,⁵⁸ V. Miftakov,⁵⁸ S. F. Schaffner,⁵⁸ A. J. S. Smith,⁵⁸ A. Tumanov,⁵⁸ E. W. Varnes,⁵⁸ G. Cavoto,⁵⁹ D. del Re,⁵⁹ R. Faccini,⁵⁹ F. Ferrarotto,⁵⁹ F. Ferroni,⁵⁹ E. Lamanna,⁵⁹ M. A. Mazzoni,⁵⁹ S. Morganti,⁵⁹ G. Piredda,⁵⁹ F. Safai Tehrani,⁵⁹ M. Serra,⁵⁹ C. Voena,⁵⁹ S. Christ,⁶⁰ R. Waldi,⁶⁰ T. Adye,⁶¹ N. De Groot,⁶¹ B. Franek,⁶¹ N. I. Geddes,⁶¹ G. P. Gopal,⁶¹ S. M. Xella,⁶¹ R. Aleksan,⁶² S. Emery,⁶² A. Gaidot,⁶² S. F. Ganzhur,⁶² P.-F. Giraud,⁶² G. Hamel Monchenault,⁶² W. Kozanecki,⁶² M. Langer,⁶² G. W. London,⁶² B. Mayer,⁶² B. Serfass,⁶² G. Vasseur,⁶² Ch. Yèche,⁶² M. Zito,⁶² M. V. Purohit,⁶³ H. Singh,⁶³ A. W. Weidemann,⁶³ F. X. Yumiceva,⁶³ I. Adam,⁶⁴ D. Aston,⁶⁴ N. Berger,⁶⁴ A. M. Boyarski,⁶⁴ G. Calderini,⁶⁴ M. R. Convery,⁶⁴ D. P. Coupal,⁶⁴ D. Dong,⁶⁴ J. Dorfan,⁶⁴ W. Dunwoodie,⁶⁴ R. C. Field,⁶⁴ T. Glanzman,⁶⁴ S. J. Gowdy,⁶⁴ T. Haas,⁶⁴ T. Himel,⁶⁴ T. Hryn'ova,⁶⁴ M. E. Huffer,⁶⁴ W. R. Innes,⁶⁴ C. P. Jessop,⁶⁴ M. H. Kelsey,⁶⁴ P. Kim,⁶⁴ M. L. Kocian,⁶⁴ U. Langenegger,⁶⁴ D. W. G. S. Leith,⁶⁴ S. Luitz,⁶⁴ V. Luth,⁶⁴ H. L. Lynch,⁶⁴ H. Marsiske,⁶⁴ S. Menke,⁶⁴ R. Messner,⁶⁴ D. R. Muller,⁶⁴ C. P. O'Grady,⁶⁴ V. E. Ozcan,⁶⁴ A. Perazzo,⁶⁴ M. Perl,⁶⁴ S. Petrak,⁶⁴ H. Quinn,⁶⁴ B. N. Ratcliff,⁶⁴ S. H. Robertson,⁶⁴ A. Roodman,⁶⁴ A. A. Salnikov,⁶⁴ T. Schietinger,⁶⁴ R. H. Schindler,⁶⁴ J. Schwiening,⁶⁴ A. Snyder,⁶⁴ A. Soha,⁶⁴ S. M. Spanier,⁶⁴ J. Stelzer,⁶⁴ D. Su,⁶⁴ M. K. Sullivan,⁶⁴ H. A. Tanaka,⁶⁴ J. Va'vra,⁶⁴ S. R. Wagner,⁶⁴ A. J. R. Weinstein,⁶⁴ W. J. Wisniewski,⁶⁴ D. H. Wright,⁶⁴ C. C. Young,⁶⁴ P. R. Burchat,⁶⁵ C. H. Cheng,⁶⁵ T. I. Meyer,⁶⁵ C. Roat,⁶⁵ R. Henderson,⁶⁶ W. Bugg,⁶⁷ H. Cohn,⁶⁷ J. M. Izen,⁶⁸ I. Kitayama,⁶⁸ X. C. Lou,⁶⁸ F. Bianchi,⁶⁹ M. Bona,⁶⁹ D. Gamba,⁶⁹ L. Bosisio,⁷⁰ G. Della Ricca,⁷⁰ L. Lanceri,⁷⁰ P. Poropat,⁷⁰ G. Vuagnin,⁷⁰ R. S. Panvini,⁷¹ C. M. Brown,⁷² P. D. Jackson,⁷² R. Kowalewski,⁷² J. M. Roney,⁷² H. R. Band,⁷³ E. Charles,⁷³ S. Dasu,⁷³ A. M. Eichenbaum,⁷³ H. Hu,⁷³ J. R. Johnson,⁷³ R. Liu,⁷³ F. Di Lodovico,⁷³ Y. Pan,⁷³ R. Prepost,⁷³ I. J. Scott,⁷³ S. J. Sekula,⁷³ J. H. von Wimmersperg-Toeller,⁷³ S. L. Wu,⁷³ Z. Yu,⁷³ T. M. B. Kordich,⁷⁴ and H. Neal⁷⁴

(The BABAR Collaboration)

¹Laboratoire de Physique des Particules, F-74941 Annecy-le-Vieux, France

²Università di Bari, Dipartimento di Fisica and INFN, I-70126 Bari, Italy

³Institute of High Energy Physics, Beijing 100039, China

⁴University of Bergen, Institute of Physics, N-5007 Bergen, Norway

⁵Lawrence Berkeley National Laboratory and University of California, Berkeley, California 94720

⁶University of Birmingham, Birmingham B15 2TT, United Kingdom

⁷Ruhr Universität Bochum, Institut für Experimentalphysik, D-44780 Bochum, Germany

⁸University of Bristol, Bristol BS8 1TL, United Kingdom

⁹University of British Columbia, Vancouver, British Columbia, Canada V6T 1Z1

¹⁰Brunel University, Uxbridge, Middlesex UB8 3PH, United Kingdom

¹¹Budker Institute of Nuclear Physics, Novosibirsk 630090, Russia

¹²University of California at Irvine, Irvine, California 92697

¹³University of California at Los Angeles, Los Angeles, California 90024

¹⁴University of California at San Diego, La Jolla, California 92093

¹⁵University of California at Santa Barbara, Santa Barbara, California 93106

¹⁶University of California at Santa Cruz, Institute for Particle Physics, Santa Cruz, California 95064

¹⁷California Institute of Technology, Pasadena, California 91125

¹⁸University of Cincinnati, Cincinnati, Ohio 45221

¹⁹University of Colorado, Boulder, Colorado 80309

²⁰Colorado State University, Fort Collins, Colorado 80523

²¹Technische Universität Dresden, Institut für Kern- und Teilchenphysik, D-01062 Dresden, Germany

²²Ecole Polytechnique, F-91128 Palaiseau, France

²³University of Edinburgh, Edinburgh EH9 3JZ, United Kingdom

²⁴Elon University, Elon University, North Carolina 27244-2010

²⁵Università di Ferrara, Dipartimento di Fisica and INFN, I-44100 Ferrara, Italy

²⁶Florida A&M University, Tallahassee, Florida 32307

²⁷Laboratori Nazionali di Frascati dell'INFN, I-00044 Frascati, Italy

²⁸Università di Genova, Dipartimento di Fisica and INFN, I-16146 Genova, Italy

²⁹Harvard University, Cambridge, Massachusetts 02138

³⁰University of Iowa, Iowa City, Iowa 52242

³¹Iowa State University, Ames, Iowa 50011-3160

³²Laboratoire de l'Accélérateur Linéaire, F-91898 Orsay, France

³³Lawrence Livermore National Laboratory, Livermore, California 94550

- ³⁴University of Liverpool, Liverpool L69 3BX, United Kingdom
³⁵University of London, Imperial College, London SW7 2BW, United Kingdom
³⁶Queen Mary, University of London, E1 4NS, United Kingdom
³⁷University of London, Royal Holloway and Bedford New College, Egham, Surrey TW20 0EX, United Kingdom
³⁸University of Louisville, Louisville, Kentucky 40292
³⁹University of Manchester, Manchester M13 9PL, United Kingdom
⁴⁰University of Maryland, College Park, Maryland 20742
⁴¹University of Massachusetts, Amherst, Massachusetts 01003
⁴²Massachusetts Institute of Technology, Laboratory for Nuclear Science, Cambridge, Massachusetts 02139
⁴³McGill University, Montréal, Quebec, Canada H3A 2T8
⁴⁴Università di Milano, Dipartimento di Fisica and INFN, I-20133 Milano, Italy
⁴⁵University of Mississippi, University, Mississippi 38677
⁴⁶Université de Montréal, Laboratoire René J.A. Lévêque, Montréal, Quebec, Canada H3C 3J7
⁴⁷Mount Holyoke College, South Hadley, Massachusetts 01075
⁴⁸Università di Napoli Federico II, Dipartimento di Scienze Fisiche and INFN, I-80126, Napoli, Italy
⁴⁹University of Notre Dame, Notre Dame, Indiana 46556
⁵⁰Oak Ridge National Laboratory, Oak Ridge, Tennessee 37831
⁵¹University of Oregon, Eugene, Oregon 97403
⁵²Università di Padova, Dipartimento di Fisica and INFN, I-35131 Padova, Italy
⁵³Universités Paris VI et VII, Laboratoire de Physique Nucléaire H.E., F-75252 Paris, France
⁵⁴Università di Pavia, Dipartimento di Elettronica and INFN, I-27100 Pavia, Italy
⁵⁵University of Pennsylvania, Philadelphia, Pennsylvania 19104
⁵⁶Università di Pisa, Scuola Normale Superiore and INFN, I-56010 Pisa, Italy
⁵⁷Prairie View A&M University, Prairie View, Texas 77446
⁵⁸Princeton University, Princeton, New Jersey 08544
⁵⁹Università di Roma La Sapienza, Dipartimento di Fisica and INFN, I-00185 Roma, Italy
⁶⁰Universität Rostock, D-18051 Rostock, Germany
⁶¹Rutherford Appleton Laboratory, Chilton, Didcot, Oxon OX11 0QX, United Kingdom
⁶²DAPNIA, Commissariat à l'Energie Atomique/Saclay, F-91191 Gif-sur-Yvette, France
⁶³University of South Carolina, Columbia, South Carolina 29208
⁶⁴Stanford Linear Accelerator Center, Stanford, California 94309
⁶⁵Stanford University, Stanford, California 94305-4060
⁶⁶TRIUMF, Vancouver, British Columbia, Canada V6T 2A3
⁶⁷University of Tennessee, Knoxville, Tennessee 37996
⁶⁸University of Texas at Dallas, Richardson, Texas 75083
⁶⁹Università di Torino, Dipartimento di Fisica Sperimentale and INFN, I-10125 Torino, Italy
⁷⁰Università di Trieste, Dipartimento di Fisica and INFN, I-34127 Trieste, Italy
⁷¹Vanderbilt University, Nashville, Tennessee 37235
⁷²University of Victoria, Victoria, British Columbia, Canada V8W 3P6
⁷³University of Wisconsin, Madison, Wisconsin 53706
⁷⁴Yale University, New Haven, Connecticut 06511

(Received 31 December 2001; published 20 May 2002)

Flavor oscillations of neutral B mesons have been studied in e^+e^- annihilation data collected with the $BABAR$ detector at center-of-mass energies near the $\Upsilon(4S)$ resonance. The data sample used for this purpose consists of events in which one B^0 meson is reconstructed in a hadronic decay mode, while the flavor of the recoiling B^0 is determined with a tagging algorithm that exploits the correlation between the flavor of the heavy quark and the charges of its decay products. From the time development of the observed mixed and unmixed final states, we determine the $B^0-\bar{B}^0$ oscillation frequency Δm_d to be $0.516 \pm 0.016(\text{stat}) \pm 0.010(\text{syst}) \text{ ps}^{-1}$.

DOI: 10.1103/PhysRevLett.88.221802

PACS numbers: 13.25.Hw, 11.30.Er, 12.15.Hh, 14.40.Nd

In the standard model, $B^0-\bar{B}^0$ mixing [1] occurs through second-order weak diagrams involving the exchange of up-type quarks, with the top quark contributing the dominant amplitude. A measurement of the mass difference Δm_d between the mass eigenstates is therefore sensitive to the value of the Cabibbo-Kobayashi-Maskawa matrix element V_{td} [2,3]. Mixing in the neutral B meson system was first seen almost fifteen years ago [4], and Δm_d

has been measured with both time-integrated and time-dependent techniques [5].

In this Letter, we present a measurement of time-dependent mixing based on a sample of 32×10^6 $B\bar{B}$ pairs recorded at the $\Upsilon(4S)$ resonance with the $BABAR$ detector at the Stanford Linear Accelerator Center. This study and a related CP asymmetry measurement [6] are described in more detail in Ref. [7]. At the PEP-II asymmetric-energy

e^+e^- collider, the $Y(4S)$ provides a source of $B^0\bar{B}^0$ pairs moving along the e^- beam direction (z axis) with a known Lorentz boost of $\beta\gamma = 0.55$, which allows a new technique for determining Δm_d with a high purity sample of fully reconstructed B^0 mesons.

The $B^0\bar{B}^0$ mixing probability, for a given B^0 lifetime τ , is a function of Δm_d and the proper decay-time difference Δt between the two neutral B mesons produced in a coherent P -wave state in the $Y(4S)$ event. The result is a time-dependent probability to observe *unmixed* (+), $B^0\bar{B}^0$, or *mixed* (-), B^0B^0 and $\bar{B}^0\bar{B}^0$, events:

$$\text{Prob}(B^0\bar{B}^0 \rightarrow B^0\bar{B}^0, B^0B^0 \text{ or } \bar{B}^0\bar{B}^0) \propto e^{-|\Delta t|/\tau} \times (1 \pm \cos\Delta m_d\Delta t). \quad (1)$$

The effect can be measured by reconstructing one B in a flavor eigenstate, referred to as B_{rec} , while the remaining charged particles originating from the decay of the other B , referred to as B_{tag} , are used to identify, or “tag,” its flavor as a B^0 or \bar{B}^0 . The charges of identified leptons and kaons are the primary indicators, although other information in the event can also be used to identify the flavor of B_{tag} . The time difference $\Delta t = t_{\text{rec}} - t_{\text{tag}} \approx \Delta z/\beta\gamma c$ is determined from the separation Δz of the decay vertices for the flavor-eigenstate and tagging B along the boost direction.

The value of Δm_d is extracted from a tagged flavor-eigenstate B^0 sample with a simultaneous unbinned maximum likelihood fit to the Δt distributions of mixed and unmixed events. There are two principal experimental complications to the probability distribution [Eq. (1)]. First, the tagging algorithm, which classifies events into categories i depending on the source of the available tagging information, incorrectly identifies the flavor of B_{tag} with a probability w_i with reduction of the observed amplitude for the oscillation by a factor $(1 - 2w_i)$. Second, the resolution for Δt is comparable to the oscillation period and must be well understood. The probability density functions for the unmixed and mixed signal events, $\mathcal{H}_{\pm, \text{sig}}$, can be expressed as the convolution of the underlying Δt distribution for the i th tagging category,

$$h_{\pm}(\Delta t; \Delta m_d, w_i) = \frac{e^{-|\Delta t|/\tau}}{4\tau} [1 \pm (1 - 2w_i) \cos\Delta m_d\Delta t],$$

with a Δt resolution function \mathcal{R} containing parameters \hat{a}_j . A log-likelihood function is then constructed by summing $\ln\mathcal{H}_{\pm, \text{sig}}$ over all events within each of the tagging categories. The likelihood is maximized to extract simultaneously the mistag rates w_i , the resolution function parameters \hat{a}_j , and the mixing parameter Δm_d .

The *BABAR* detector is described in detail elsewhere [8]. Charged particles are detected and their momenta measured by a combination of a 40-layer drift chamber (DCH) and a five-layer silicon vertex tracker (SVT) embedded in a 1.5-T solenoidal magnetic field. A detector of internally reflected Cherenkov radiation (DIRC) is used

for charged hadron identification. Kaons are identified with a neural network based on the likelihood ratios in the SVT and DCH, derived from dE/dx measurements, and in the DIRC, calculated by comparing the observed and expected pattern of Cherenkov light for either kaons or pions. A finely segmented CsI(Tl) electromagnetic calorimeter (EMC) is used to detect photons and neutral hadrons, and to identify electrons. Electron candidates are required to have a ratio of EMC energy to track momentum, an EMC cluster shape, DCH dE/dx , and DIRC Cherenkov angle consistent with expectation. The instrumented flux return (IFR) contains resistive plate chambers for muon and neutral hadron identification. Muon candidates are required to have IFR hits located along the extrapolated DCH track, an IFR penetration length, and an energy deposit in the EMC consistent with the muon hypothesis.

Neutral B mesons are reconstructed in a sample of multihadron events in the flavor eigenstate decay modes $D^{(*)-}\pi^+$, $D^{(*)-}\rho^+$, $D^{(*)-}a_1^+$, and $J/\psi K^{*0}$. The decay channels $K^+\pi^-$, $K^+\pi^-\pi^0$, $K^+\pi^+\pi^-\pi^-$, and $K_S^0\pi^+\pi^-$ are used to reconstruct \bar{D}^0 candidates, while the modes $K^+\pi^-\pi^-$ and $K_S^0\pi^-$ are used for D^- candidates. Charged D^{*-} candidates are formed by combining a \bar{D}^0 with a soft π^- . Finally, the B^0 candidates are formed by combining a D^{*-} or D^- candidate with a π^+ , ρ^+ ($\rho^+ \rightarrow \pi^+\pi^0$), or a_1^+ ($a_1^+ \rightarrow \pi^+\pi^-\pi^+$); likewise, $B^0 \rightarrow J/\psi K^{*0}$ candidates are reconstructed from combinations of J/ψ candidates, in the decay modes e^+e^- and $\mu^+\mu^-$, with a K^{*0} ($K^{*0} \rightarrow K^+\pi^-$). The selection and reconstruction of these decays is described in detail in Ref. [9].

Neutral B candidates are identified by the difference ΔE between the energy of the candidate and the beam energy $\sqrt{s}/2$ in the center-of-mass frame, and the beam-energy substituted mass m_{ES} , calculated from $\sqrt{s}/2$ and the reconstructed momentum of the B candidate. Candidates are selected by requiring $m_{\text{ES}} > 5.2 \text{ GeV}/c^2$ and ΔE within ± 2.5 standard deviations of 0 (typically $|\Delta E| < 40 \text{ MeV}$). When multiple candidates in a given event are selected (with probability of about 0.25%), only the one with the smallest $|\Delta E|$ is retained.

After the daughter tracks of the B_{rec} are removed, the remaining tracks are analyzed to determine the flavor of the B_{tag} . Events are assigned a lepton tag if they contain an identified lepton with a center-of-mass momentum greater than 1.0 or 1.1 GeV/c for electrons and muons, respectively, thereby selecting mostly primary leptons. If the sum of charges of all identified kaons is nonzero, the event is assigned a kaon tag. The final two tags involve a multivariable analysis based on a neural network, which is trained to identify primary leptons, kaons, and soft pions, and the momentum and charge of the track with the maximum center-of-mass momentum. Depending on the output of the neural net, events are assigned either an NT1 (more certain) tag, an NT2 (less certain) tag, or are not tagged at all (about 30% of all events) and excluded from the analysis.

Tagging assignments are made mutually exclusive by the hierarchical use of the tags. Events with a lepton tag and no conflicting kaon tag are assigned to the lepton category. If no lepton tag exists, but the event has a kaon tag, it is assigned to the kaon category. Otherwise, events with neural network tags are assigned to corresponding neural network categories.

The decay time difference Δt between B decays is determined from the measured separation $\Delta z = z_{\text{rec}} - z_{\text{tag}}$ along the z axis between the reconstructed $B_{\text{rec}}(z_{\text{rec}})$ and flavor-tagging decay $B_{\text{tag}}(z_{\text{tag}})$ vertex. This measured Δz is converted into Δt with the use of the known $Y(4S)$ boost, including a correction on an event-by-event basis for the direction of the B mesons with respect to the z direction in the $Y(4S)$ frame. The Δt resolution is dominated by the z resolution of the tag vertex position. After removal of the B_{rec} daughters, the B_{tag} vertex is formed from all remaining tracks in the event except kaons, which are mostly D meson decay products. An additional constraint is provided by the calculated B_{tag} production point and three momentum, determined from the momentum of the B_{rec} candidate, its decay vertex, the average position of the interaction point, and the $Y(4S)$ boost. Tracks with a large contribution to the χ^2 are iteratively removed until those remaining (≥ 1) have a reasonable fit probability or all tracks are removed. Only events with a reconstructed B_{tag} vertex, $|\Delta t| < 20$ ps and $\sigma_{\Delta t} < 1.4$ ps are retained (about 84%), where $\sigma_{\Delta t}$ is the measurement error derived from the vertex fits.

The distribution of m_{ES} for the selected candidates is shown in Fig. 1, where the result of a fit with a Gaussian distribution for the signal and an ARGUS function [10] for the background is also displayed. The fitted number of signal events and their purity (for $m_{\text{ES}} > 5.27$ GeV/c^2) are 6347 ± 89 and $(85.8 \pm 0.5)\%$, respectively. The sample composition by tagging category is given in Table I.

In the likelihood fit, the Δt resolution function is approximated by a sum of three Gaussian distributions (core, tail, and outlier) with different means and widths,

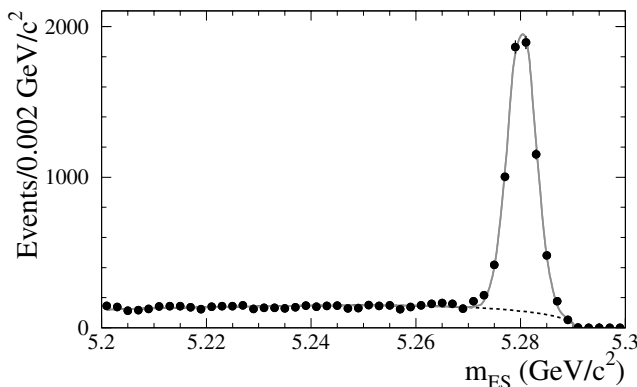


FIG. 1. Distribution of m_{ES} for all B^0 candidates with a flavor tag and a reconstructed tag vertex.

$$\mathcal{R}(\delta_t; \hat{a}) = \sum_{k=1}^2 \frac{f_k}{S_k \sigma_{\Delta t} \sqrt{2\pi}} \exp\left(-\frac{(\delta_t - b_k \sigma_{\Delta t})^2}{2(S_k \sigma_{\Delta t})^2}\right) + \frac{f_3}{\sigma_3 \sqrt{2\pi}} \exp\left(-\frac{\delta_t^2}{2\sigma_3^2}\right),$$

where $\delta_t = \Delta t - \Delta t_{\text{true}}$. The sum of the fractions f_k is constrained to unity. For the core and tail Gaussians, the widths $\sigma_k = S_k \times \sigma_{\Delta t}$ are the event-by-event measurement errors multiplied by overall scale factors S_k . The scale factor of the tail Gaussian is fixed to the Monte Carlo value since it is strongly correlated with the other resolution function parameters. The third Gaussian, with a fixed width of $\sigma_3 = 8$ ps, accounts for outlier events with incorrectly reconstructed vertices (less than 1% of events). A separate core bias coefficient $b_{1,i}$ is allowed for each tagging category i to account for small shifts due to inclusion of charm decay products in the tag vertex, while a common bias coefficient b_2 is used for the tail component. These offsets are proportional to $\sigma_{\Delta t}$ since both the size of the bias and the resolution for z_{tag} depend kinematically on the polar angle of the flight direction of the charm daughter. The tail and outlier fractions and the scale factors are assumed to be the same for all decay modes, since the z_{tag} measurement dominates the resolution for Δt . This assumption is confirmed by Monte Carlo studies. Separate resolution parameters are used for two different data-reconstruction periods, referred to as Run1 and Run2, which mainly differ in vertex performance and tracking efficiency.

In the presence of backgrounds, which are dominated by continuum e^+e^- and $B\bar{B}$ combinatorial sources, additional terms are added to the signal PDF $\mathcal{H}_{\pm, \text{sig}}$ for various background types,

$$\mathcal{H}_{\pm, i} = f_{i, \text{sig}} \mathcal{H}_{\pm, \text{sig}} + \sum_{j=\text{bkgd}} f_{i, j} \mathcal{B}_{\pm, i, j}(\Delta t; \hat{b}_{\pm, i, j}),$$

where the background PDFs $\mathcal{B}_{\pm, i, j}$ provide an empirical description for the possible Δt behavior of background events in each tagging category i . The background Δt types considered are a zero lifetime component and a nonoscillatory component with an empirical nonzero lifetime. We fit for separate resolution function parameters for signal and background to minimize correlations. The fraction of background events for each tagging category and background source is given by $f_{i, j}$, while $\hat{b}_{\pm, i, j}$ are parameters used to characterize each source of background

TABLE I. Signal yields per tagging category, obtained from the m_{ES} distributions after all selection requirements. The purity is quoted for $m_{\text{ES}} > 5.27$ GeV/c^2 .

Category	Tagged	Purity (%)
lepton	1097 ± 34	96.0 ± 0.7
kaon	3156 ± 63	84.6 ± 0.7
NT1	798 ± 31	88.9 ± 1.2
NT2	1293 ± 43	79.4 ± 1.3

by tagging category for mixed and unmixed events. The signal probability $f_{i,\text{sig}}$ is determined from the measured event m_{ES} on the basis of a separate fit to the observed m_{ES} distribution in tagging category i . The sum of signal and background fractions is forced to unity.

Altogether, the likelihood fit involves a total of 44 parameters, including Δm_d , the average mistag fraction and the difference between B^0 and \bar{B}^0 for each tagging category (8), parameters for the signal Δt resolution (16), and parameters for background time dependence (5), Δt resolution (6), and effective dilutions (8). The value of Δm_d was kept hidden throughout the analysis until all analysis details and the systematic errors were finalized, to eliminate possible experimenter's bias.

The results from the likelihood fit to the tagged B^0 sample are summarized in Table II. The probability to obtain a likelihood smaller than that observed is 44%, evaluated with a parametrized Monte Carlo technique. The value of Δm_d given by the fit, prior to final corrections, is $\Delta m_{d,\text{fit}} = 0.525 \pm 0.016 \text{ ps}^{-1}$. One method for displaying the result of the full likelihood fit is to use the observed mixing asymmetry,

$$\mathcal{A}_{\text{mix}}(\Delta t) = \frac{N_{\text{unmixed}}(\Delta t) - N_{\text{mixed}}(\Delta t)}{N_{\text{unmixed}}(\Delta t) + N_{\text{mixed}}(\Delta t)}.$$

The unit amplitude for the otherwise pure cosine dependence of \mathcal{A}_{mix} is diluted by the mistag probability and the experimental resolution for Δt . The observed Δt distributions of both the mixed and unmixed events, and their asymmetry \mathcal{A}_{mix} , are shown along with projections of the likelihood fit result in Fig. 2.

Since the parameters of the Δt resolution for both signal and backgrounds are free parameters in the fit, their contribution to the uncertainty on Δm_d is included as part of the statistical error. Remaining systematic errors arise from the choice of the signal Δt resolution description, its capability to handle outliers and various worst-case SVT misalignment scenarios ($\pm 0.005 \text{ ps}^{-1}$), and by approximations and uncertainties in the Δz to Δt conversion from the absolute z scale of the detector and PEP-II boost (less than $\pm 0.002 \text{ ps}^{-1}$). Systematic errors due to background include the choice of its Δt distribution and resolution description ($\pm 0.002 \text{ ps}^{-1}$), variation of the sum of background fractions from the separate m_{ES} fits, and the uncertainty on the magnitude of the small B^+ component of

TABLE II. Results for Δm_d and a subset of the parameters obtained from the likelihood fit to the Δt distributions. Δm_d includes small corrections described in the text.

Parameter	Fit value	Parameter	Fit value
Δm_d	0.516 ± 0.016		
w (Lepton)	0.079 ± 0.014	w (NT1)	0.219 ± 0.022
w (Kaon)	0.166 ± 0.012	w (NT2)	0.344 ± 0.020
S_1 (Run1)	1.37 ± 0.09	S_1 (Run2)	1.18 ± 0.11
f_2 (Run1)	0.014 ± 0.020	f_2 (Run2)	0.015 ± 0.010
f_3 (Run1)	0.008 ± 0.004	f_3 (Run2)	0.000 ± 0.014

the signal ($\pm 0.002 \text{ ps}^{-1}$). A correction of -0.002 ps^{-1} , derived from data, is made to account for the small variation of the background composition as a function of m_{ES} , which affects the background Δt distribution. The statistical error ($\pm 0.002 \text{ ps}^{-1}$) on this correction is included as a systematic uncertainty. An additional correction of -0.007 ps^{-1} is applied for a bias observed in fully simulated Monte Carlo events. The bias is mainly due to correlations between the mistag rate and the Δt resolution that are not explicitly incorporated into the likelihood function. The systematic error assigned to this correction includes contributions from the statistical precision of the Monte Carlo study ($\pm 0.003 \text{ ps}^{-1}$), model variations due to uncertain branching fractions and lifetimes of the tag-side D mesons and the assumed fraction of wrong-sign kaons produced in B decays ($\pm 0.001 \text{ ps}^{-1}$), and variation of the requirement on the maximum allowed value of $\sigma_{\Delta t}$ ($\pm 0.003 \text{ ps}^{-1}$). Finally, the variation of the fixed B^0 lifetime within the known errors [5] leads to a systematic uncertainty of $\pm 0.006 \text{ ps}^{-1}$.

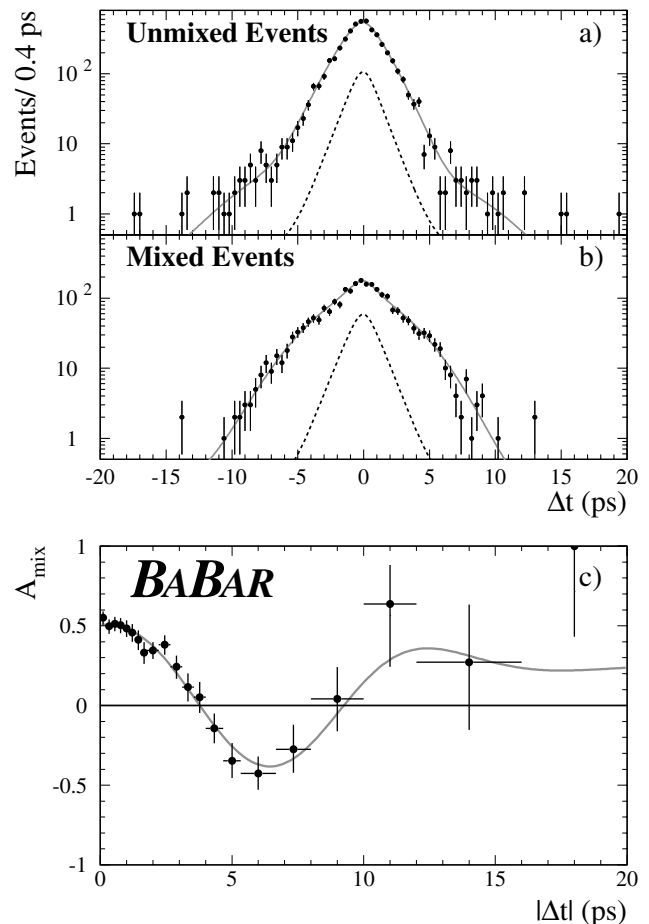


FIG. 2. Distributions of Δt data for the selected (a) unmixed and (b) mixed events [$m_{\text{ES}}(B_{\text{rec}}) > 5.27 \text{ GeV}/c^2$], with projections of the likelihood fit (solid) and the contribution of the background (dashed) overlaid. The time-dependent mixing asymmetry $\mathcal{A}_{\text{mix}}(|\Delta t|)$ is shown in (c).

In conclusion, a new technique involving the time-difference distribution of a tagged sample of fully reconstructed neutral B decays has been used to determine the $B^0\text{-}\bar{B}^0$ mixing frequency Δm_d to be

$$\Delta m_d = 0.516 \pm 0.016(\text{stat}) \pm 0.010(\text{syst}) \text{ ps}^{-1}.$$

This is one of the single most precise measurements available, with an error still dominated by the sample size. The sample consists almost entirely of neutral B mesons, with excellent control of both flavor tagging for the recoil B and measurement of the vertex separation between reconstructed and tagged B meson. The result is consistent with the current world average [5] and a recent $BABAR$ measurement with a dilepton sample [11]. The analysis shares the same flavor-eigenstate sample, and tagging and vertexing algorithms as used for the determination of $\sin 2\beta$, thereby providing an essential validation for the reported $\sin 2\beta$ result [6].

We are grateful for the excellent luminosity and machine conditions provided by our PEP-II colleagues, and for the substantial dedicated effort from the computing organizations that support $BABAR$. The collaborating institutions thank SLAC for its support and kind hospitality. This work is supported by DOE and NSF (U.S.A.), NSERC (Canada), IHEP (China), CEA and CNRS-IN2P3 (France), BMBF (Germany), INFN (Italy), NFR (Norway), MIST (Russia),

and PPARC (United Kingdom). Individuals have received support from the A. P. Sloan Foundation, Research Corporation, and Alexander von Humboldt Foundation.

*Also with Università di Perugia, Perugia, Italy.

†Also with Università della Basilicata, Potenza, Italy.

- [1] The symbol B^0 refers to the B_d meson; charge conjugate modes are implied throughout this paper.
- [2] N. Cabibbo, Phys. Rev. Lett. **10**, 531 (1963); M. Kobayashi and T. Maskawa, Prog. Theor. Phys. **49**, 652 (1973).
- [3] For a recent discussion of the relation, see C. Gay, Annu. Rev. Nucl. Part. Sci. **50**, 577 (2000).
- [4] UA1 Collaboration, C. Albajar *et al.*, Phys. Lett. B **186**, 247 (1987); ARGUS Collaboration, H. Albrecht *et al.*, Phys. Lett. B **192**, 245 (1987).
- [5] D. E. Groom *et al.*, Eur. Phys. J. C **15**, 1 (2000).
- [6] $BABAR$ Collaboration, B. Aubert *et al.*, Phys. Rev. Lett. **87**, 151802 (2001).
- [7] $BABAR$ Collaboration, B. Aubert *et al.*, $BABAR\text{-PUB-01/03}$, hep/ex-0201020, Phys. Rev. D (to be published).
- [8] $BABAR$ Collaboration, B. Aubert *et al.*, Nucl. Instrum. Methods Phys. Res., Sect. A **479**, 1 (2002).
- [9] $BABAR$ Collaboration, B. Aubert *et al.*, Phys. Rev. Lett. **87**, 201803 (2001).
- [10] ARGUS Collaboration, H. Albrecht *et al.*, Phys. Lett. B **241**, 278 (1990).
- [11] $BABAR$ Collaboration, B. Aubert *et al.*, following Letter, Phys. Rev. Lett. **88**, 221803 (2002).